

Article

Coastal Defence Integrating Wave-Energy-Based Desalination: A Case Study in Madagascar

Pasquale Contestabile ^{1,2,*} and Diego Vicinanza ^{1,2,3} 

¹ Department of Engineering, University of Campania “Luigi Vanvitelli”, via Roma, 29, 81031 Aversa (Caserta), Italy; diego.vicinanza@unicampania.it

² Inter-University National Consortium for Marine Sciences (CoNISMa), Piazzale Flaminio, 9-00196 Roma, Italy

³ Stazione Zoologica Anton Dohrn; Villa Comunale, 80121 Napoli, Italy

* Correspondence: pasquale.contestabile@unicampania.it

Received: 10 April 2018; Accepted: 25 May 2018; Published: 1 June 2018



Abstract: In arid, coastal cities, water demand is often met through large-scale desalination systems. However, the energy required to run desalination plants remains a drawback. Further, numerous low-density population areas lack not only fresh water availability, but in most of the cases electrical grid connection or any other energy source as well. The challenge, consequently, is to ensure adequate fresh water supplies at the lowest possible cost. The main objective of this work is to assess the freshwater production from a reverse osmosis desalination system powered by a wave energy converter, the Overtopping Breakwater for Wave Energy Conversion (OBREC). The desktop analysis is illustrated through a case study on the Fenoarivo Atsinanana coast, along north-eastern Madagascar. The novel aspect of the analysis method is the application of a specific numerical code calibrated using preliminary results from a two-year monitoring campaign of the first OBREC prototype in operation in Naples Harbour (Italy). Instead of dissipating the incoming wave energy, the system collects the overtopping water above the sea level and the potential energy is converted into electricity through low head turbines. Then, the flow will be driven towards the desalination system. This configuration seems like a promising opportunity for developing countries to meet their water supply needs while at the same time developing their renewable energy potential.

Keywords: desalination; wave energy; OBREC; green ports

1. Introduction

Today, over 1.76 billion people live in places with a high degree of water shortage, since they do not have access to freshwater, or, if they have, such water is unable to be used [1]. Due to the unfair distribution of water resources in the world, the quality and the quantity of water are not sufficient to ensure minimum conditions of wellness in several countries, first and foremost the African countries facing the ocean. Here, many cities and small villages along the coastline are experiencing a real freshwater crisis, but at the same time have abundant salt water sources. This difficulty in providing water has caused many countries in the world to look for new water sources, and to find in seawater desalination a valid alternative to alleviate this crisis situation. Data supplied by the International Desalination Association for the year 2015 [2], show that the total number of desalination plants installed was 18,426, serving more 300 million people in 150 countries throughout the world. The global capacity is more than 86.8 million m³/day, and about 60% of the feed water used is seawater [2].

Like any other water treatment technology or separation processes, seawater desalination, requires the use of energy to produce freshwater. However, numerous low-density population areas

lack not only fresh water availability, but in most of the cases electrical grid connection or any other energy source as well. For such locations, the energy required to run desalination plants remains a drawback. The challenge, consequently, is to ensure adequate and sustainable fresh water supplies at the lowest possible economic and environmental cost. Renewable-energy-powered desalination represents a key enabler for continued growth, especially for those regions that rely on desalinated water to sustain local communities and for productive uses such as irrigation. This approach could substantially contribute to reducing the fossil fuels use and the associated CO₂ released [3–5]. Furthermore, due to the fact that fossil fuel prices are very variable, with an upward trend, the use of alternative energies is a valid alternative that permits the reduction of risks concerning energy price increases during the life cycle of the desalination device [6].

From a technical point of view, two main categories can be used to classify salt separation technologies: thermal desalination (multi-phase change processes) and membrane process separation (single-phase processes). The first includes: multistage flash (MSF), multiple effect distillation (MED) and vapour compression (VC). The second category covers electro dialysis (ED) processes and reverse osmosis (RO) [7]. More recently, a third category is emerging as combination of the two, such as hybrid technologies in which a pre-treatment phase is provided by membrane separation and a secondary treatment is carried out by thermal desalination or vice versa [8]. A joint study by the International Renewable Energy Agency (IRENA) and the International Energy Agency (IEA) [9] in 2012 stated that the dominant process on the market was reverse osmosis, covering over 60% of the total commissioned plants.

A first example of technologies that combine a wave energy converter (WEC) and a desalination process was based on the pioneer Salter duck and consists of vapour compression equipment inside a floating duck [10]. The first RO technology combined in a WEC was called Delbuoy, an oscillating buoy to drive a piston pumps that fed seawater to submerged RO modules [11,12]. The device produced about 2 m³/day. Although the system worked successfully for 18 months, the project did not continue due to the inefficiency of the oscillating buoy in converting wave energy [10,13]. Another technology was installed at Vizhinjam, India in 1990, consisting of an oscillating water column device coupled to a diesel generator, alternatively used according to sea conditions [14]. For several wave energy converters (AquaBuoy, McCabe Wave Pump, OMI Wave Pump, CETO) the coupling with desalination by reverse osmosis have been proposed, even if without going into the details [15–17]. The world's first commercial-scale wave energy was lastly installed in Perth, Australia, connected to the electricity grid and used for desalination plant [18].

Hence, it is noticeable that RO is the most commonly used technique for the previous tentative production of desalinated water combined with wave energy devices. The main reason for this could be the high development level of such technology, which represents one of the most efficient process for water with high concentrations (above 35,000 ppm) of total dissolved solids [19]. Ongoing simulations and future analysis will also benefit some emerging hybrid technologies, i.e., integrated RO–ED process, in which the electro dialysis process is applied firstly, followed by reverse osmosis [20]. However, in order to set pragmatic simulations under the current market scenario, the analysis presented in this paper refers to an existing RO machine. This desktop study, hence, assesses the efficacy of using wave energy to power a desalination plant through a demonstration site in North-East Madagascar.

2. Materials and Methods

2.1. Objectives and Approach

The identification of a site-specific design for a renewable energy-driven desalination plant is a very complex process and a detailed feasibility analysis is required.

Obviously, the first stage of a pre-feasibility analysis is characterized by a quantitative assessment of the freshwater production, which is the focus of this study. Hence, the presented analysis disregards

the nature conservation aspects, non-technical barriers and other matters included in the environmental impact assessment.

2.2. Area Overview

Madagascar is one of the poorest countries in the world, with a population growing faster than its economy [21]. Over 11 million people do not have access to clean and safe water and almost 4000 children under five die every year from diarrheal diseases caused by unsafe water and poor sanitation (wateraid.org). The site considered in the present work is Fenoarivo Atsinanana, the capital of the Analanjirofo region and of the Fenoarivo Atsinanana District, located on the east coast (Figure 1). Although the region has plenty of water, it carries diseases such as malaria. Fenoarivo is 186 nautical miles (345 km) from the port of Antalaha and 56 nautical miles (103 km) from the port of Toamasina, which are the nearest harbours. For this reason, i.e., the absence of a port along a coast for about 400 km, the realization of an harbour at sites such as this has been suggested [22]. Therefore, the hypothesis of a new port breakwater is considered in the following. The details of this infrastructure or the structural design criteria are beyond the scope of the present paper. Moreover, from the perspective that nothing is worse than a water scarcity, environmental issues or non-technical barriers shall not be discussed further. The main aim of the study is to assess the potential of an overtopping-device-based desalting plant in an effectively disadvantaged context.

The main work hypotheses are:

- the analyzed main breakwater integrating the desalination modules is designed to connect the two natural reefs, for a length of 500 m, as shown in Figure 1;
- the orientation is 15.0° N, i.e., approximately orthogonal to the main wave sector, as discussed below;
- the average depth is 5 m;
- the connection to the electric grid and the water network is provided by bottom-set service lines. If a secondary breakwater is required (to create the port basin), it could be equipped with these services.

2.3. Overtopping Breakwater for Wave Energy Conversion

The Overtopping Breakwater for Energy Conversion (OBREC) is a highly-developed overtopping wave energy converter (OTD) totally integrated into an existing rubble mound breakwater. Its first prototype was installed in the Naples harbour at the end of 2015 with the aim of moving from the traditional approach of a dissipative coastal defence to a new, “green” structure that captures the incoming waves (Figure 2). The device collects the overtopping water above the sea level by means of a robust concrete reservoir. Then, the flow is driven towards low head turbines to generate a more useful form of energy, i.e., electricity. All the electro-mechanical devices, installed behind the OBREC crown wall, are safe from the direct action of waves, increasing the reliability of the system (Figure 3). Thanks to site-specific turbine strategy, including several pico turbines (<5 kW) or a combination of pico and micro turbines (<100 kW), OBREC works with a wide spectrum of different incident wave conditions and water levels. The device tends to be most effective in mild and poor wave climates [23–26].



Figure 1. Map of the north-eastern Madagascar coasts showing the location of the analysed OBREC installation at Fenoarivo Atsinanana.



Figure 2. The 6 m wide OBREC prototype operating at the Port of Naples (Italy), integrated into the main breakwater with an ANTIFER-type armour layer.

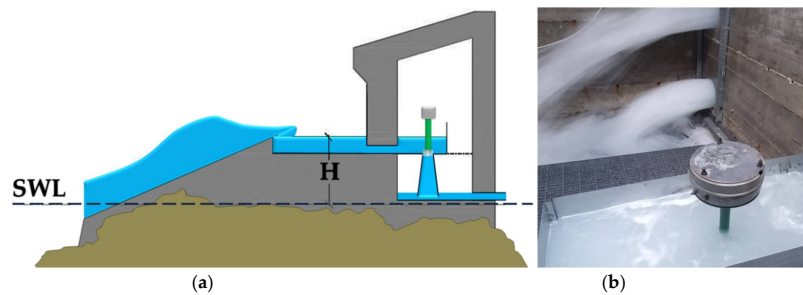


Figure 3. (a) OBREC’s working principle, with an overtopping ramp, reservoir and pico-turbine inside the machine room; (b) a pico-turbine installed in the engine room, and a water jet derived by the flow rate in front of the crown wall.

2.4. Wave Climate

2.4.1. Wave Dataset

The dataset used is provided by the European Centre for Medium-Range Weather Forecasts (ECMWF) [27]. The ECMWF is an independent intergovernmental organisation supported by 34 states that produces and disseminates numerical weather predictions to its member states. The centre is a meteorological data assimilation project where an atmosphere circulation reanalysis is integrated with the WAVE Model (WAM), a third generation ocean wave prediction model. Weather predictions are based on the implementation of weather observations collected over decades through a single consistent analysis in forecast models. The dataset used is a global atmospheric reanalysis defined as ERA-Interim, in operation since January 1979. The WAM provides 6-h values of significant wave height (H_s), mean wave period (T_m) and mean wave direction (θ_m). From a 20-year dataset, ranging from July 1998 to July 2017, the offshore average wave power was computed by using the approximate deep water expression for the wave energy flux, P , as follows

$$P = \frac{\rho \times g^2 \times H_{m0}^2 \times T_e}{64 \times \pi} \quad (1)$$

where ρ and g are respectively the sea water density and the gravity acceleration, H_{m0} is the wave height computed on the zero-order moment of spectral function, and T_e is the wave energy period [28]. Since the ECMWF provides values for T_m , the energy period was assumed as $1.14 T_m$ [23,24,29,30]. For the area related to Fenoarivo Atsinanana, the chosen point from the ECMWF grid has the coordinates -17.25° S and 50.25° E, which are better described in the following sections.

2.4.2. Wave Propagation

The assessment of the realistic prospective of energy production in the selected area was carried out by means of the numerical suite Mike 21 SW spectral wave model, developed by DHI Water and Environment [31]. The code is a stationary, directionally decoupled, parametric model that takes into account the effects of refraction and shoaling due to varying depths, local wind generation and energy dissipation due to bottom friction and wave breaking. The basic equations in the model are derived from the conservation equation for the spectral wave action density [32]. The implicit assumption is that water depth, wave and current fields vary on space and time scales that are much larger than the variation scales of single properties of the medium. A parameterization of the conservation equation in the frequency domain is performed by introducing the zeroth and the first moment of the action spectrum as dependent variables. The MIKE 21 SW lateral boundary conditions were considered symmetrical. A high resolution grid was used to provide reliable estimates of wave power in coastal waters. This grid was characterized by a linearly variable resolution between 750 m to 150 m for depths in the range 500 m to 100 m. Constant values of 150 m and 1000 m of

the grid resolution were assumed respectively for water depths shallower than 100 m and deeper than 500 m, respectively. The seabed was performed by interpolating at the grid nodes the latest release of the 30 arc-second global bathymetric grid provided by the General Bathymetric Chart of the Oceans (GEBCO) database [33]. To accurately define wave patterns in really shallow water, detailed bathymetry is required. Therefore, for depths less than 10 m, the GEBCO charts were implemented by manually inserting nautical information obtained from Navionics [34].

The given waves were propagated from depths of 1000–3500 m to depths of 5 m. Wave power series were calculated from the resulting dataset provided by the transformation model. In fact, for each nearshore wave the corresponding energy period was computed, in order to allow the calculation of the related power value by Equation (1). The energy density results are based, hence, on the 30-year average.

2.5. Performance Analysis

2.5.1. Energy Production

Traditionally, the energy production of a WEC is estimated by the power matrix, i.e., crossing the incident wave conditions with the expected power. Since the monitoring of the OBREC has just begun, no definitive power matrix is available. Hence, the power efficiency parameters are computed by means of a specifically-designed numerical model, called OBRECsim (Figure 4). The software provides detailed modelling of the OBREC hydrodynamics because a well-specified overtopping flow rate formula provided by an OBREC small-scale laboratory test [35], has been implemented. Moreover, the preliminary results obtained during a two-year monitoring campaign of the full-scale OBREC prototype were used to calibrate the code. These results refer especially to hydro-electromechanical equipment efficiency, turbine strategies (i.e., start/stop strategies and turbine coupling) and power take-off efficiency.

The modelling of hydrodynamics inside the reservoir consider the unsteady water flow through the channel. The basic computational procedure for steady flow is based on the solution of the one-dimensional energy equation. Energy losses are evaluated by friction and contraction/expansion. The momentum equation may be used in situations where the water surface profile is rapidly varied. For unsteady flow, OBRECsim solves the full dynamic one-dimensional Saint-Venant equation using an implicit, finite difference method.

The aim of the simulation was to determine the optimal geometry of the device and the turbine strategy for which the energy production is maximized. The input parameters were:

- wave characteristics of sea states;
- tentative geometry of the device;
- tentative turbine configuration.

Operatively, the waves from the 20-year averaged 6-h triple dataset for the nearshore wave climate at the study site were grouped by classes of $H_s-T_p-\theta_m$. In order to estimate the electricity production, the code simulates a time series of the mean water flow passing through the turbines, $Q_{RESERVOIR}$. The numerical model is based on the continuity equation:

$$Q_{RESERVOIR} = Q_{IN} - Q_{REAR} - Q_{OVERFLOW} \quad (2)$$

where:

- $Q_{RESERVOIR}$ is the flow through the turbines;
- Q_{IN} is the total overtopping flow rate, as provided by Iuppa et al. [35];
- Q_{REAR} is the overtopping flow rate at the rear side of the structure;
- $Q_{OVERFLOW}$ is the outgoing reflected flow when the reservoir is saturated.

The overall efficiency of the system, η_{OBREC} , is described as the product of the levels of efficiency as follows:

$$\eta_{OBREC} = \eta_{RAMP} \times \eta_{RESERVOIR} \times \eta_{TURBINES} \times \eta_{EQUIPMENTS} \tag{3}$$

in which

- η_{RAMP} is the efficiency of the ramp, i.e., the rate of total incident power overtopping the crests;
- $\eta_{RESERVOIR}$ represents the efficiency of the reservoir, in terms of the potential energy stored or lost to overflow in the reservoirs;
- $\eta_{TURBINES}$ refers to turbine efficiency, as potential energy is transformed into kinetic energy by the turbines and is related to start/stop penalties;
- $\eta_{EQUIPMENTS}$ defines the electromechanical efficiency, as power take-off and generator efficiency and inverter losses.

In order to estimate the energy production, the efficiency curve of a kind of turbine actually installed on the prototype was taken into account in the present analysis. The pico-turbine model used in the simulations is the propeller type ZD760-LM-20, provided by ELECTWAY [36]. The nominal power is 1 kW for an hydraulic head of 1.5 m and an mean flow rate of about 100 L/s. This turbine was selected as it is the larger model of a couple of propellers actually installed on the prototype, making it a well-known technology [23]. Therefore, an accurate efficiency curve was adopted within the OBRECsim code. In particular, a maximum efficiency of 73.2% at the nominal flow rate was imposed on the hydro-electrical system.

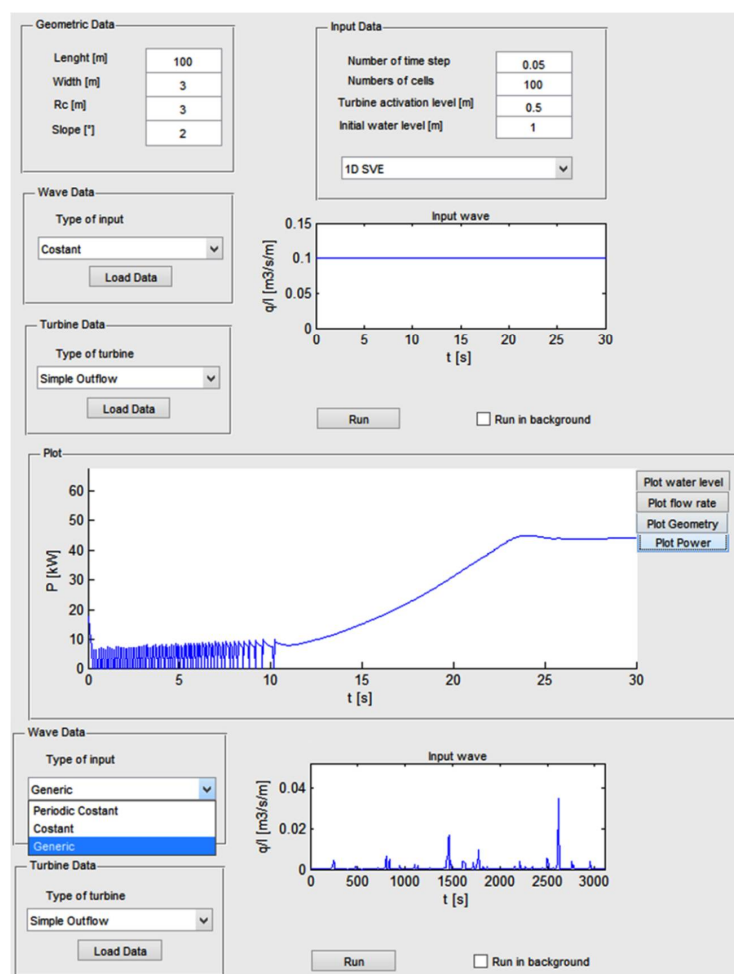


Figure 4. The OBRECsim program with a newly-initiated simulation list.

2.5.2. Freshwater Production

The energy production computations were used to force a numerical simulation by which the amount of desalinated water was estimated. The major energy required for desalting is for pressurizing the feed water [37]. This process is based on the osmosis principle; osmosis is a natural phenomenon that occurs in water, which, when penetrating a semi-permeable membrane, passes from a lower salt concentration solution to a more concentrated solution. When pressure is applied to the more concentrated solution (that overcomes the osmotic pressure), water starts to flow through the membrane in the opposite direction. This is called the reverse osmosis process [38].

The analysis took into account a well-established RO system technology, so as to examine a clear pattern of freshwater production and the related power demand.

Figure 5 describes the overall scheme of the seawater RO plant specifically modified for the OBREC application. In this configuration, in fact, wave overtopping provides the saline feedwater and the main source of electricity. The major stages considered in the scheme are summarised in the following.

- The overtopping water is accumulated in the reservoir through the wave overtopping principle and creates a head difference between the water inside the reservoir and the mean sea water level. The head difference generates a flow, which runs a turbine in order to produce electricity. From the bottom of the engine room, a percentage of 10–15% of the total outflow is then redirected for pre-treatment by a small pump operating at about 2 bar, while the remaining water returns directly to the sea.
- The electricity produced by the turbines is stabilized. Moreover, only a percentage of the total amount of electricity produced is consumed by the producer. In fact, in storm conditions, i.e., when the energy production is greater than the electricity required to run the desalination system, the power is exported to the grid or collected in a storage system.
- The water is pre-treated to remove all suspended solids and all the constituents that can cause fouling. Pre-treatment is based on filtration and chemical addition. Alternative pre-treatment could be achieved by the use of a beach drainage technique, for which the sand acts as a natural filter, while dewatering of the swash zone is achieved for beach erosion control [39–42].
- The produced electricity supplies the energy for the pre-treatment and the high pressure (60–65 bar) pumping system, the reverse osmosis process and the post-treatment unit.
- Desalination produces two streams: one with low concentrations of salts and one with higher salt concentrations than the feed water. This second stream is traditionally called brine. Normally, the “recovered” brine is about 40–50% of the total feedwater driven into the RO system.
- Connected to the RO system there is an energy recovery device, including a flow control centre including concentrated and recycled valves. Such machines are designed to recover the hydraulic energy of the pressurized water flow. The average efficiency values are around 40–60%.
- The last step for the water is post-treatment, in which the water is prepared for distribution. The processes include:
 - Remineralization with lime materials and carbon dioxide;
 - PH adjustment to a range of 6.8 to 8.1;
 - Disinfection using bromide- and iodide-based products.

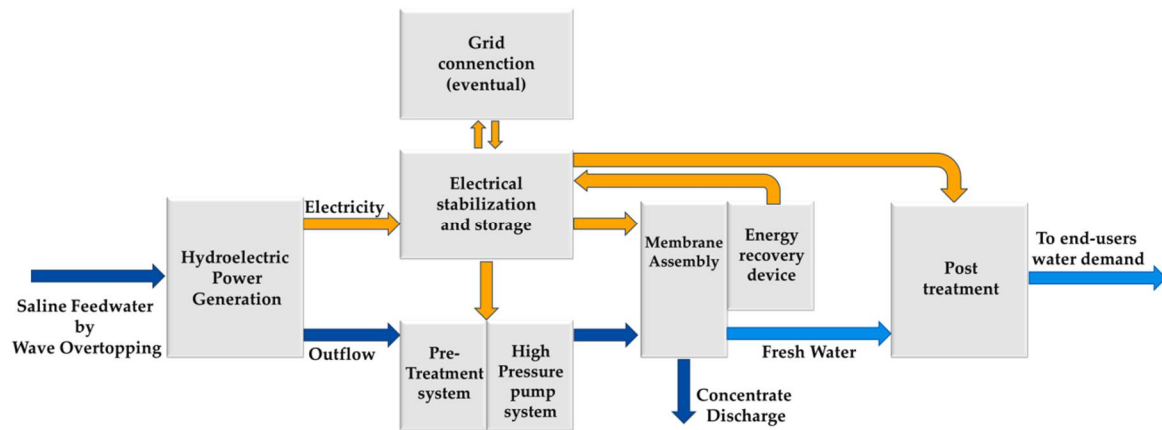


Figure 5. Scheme of the reverse osmosis plant embedded in the OBREC system.

The seawater desalination machine specifically considered in the analysis is the SeaPRO-16,35K,380,TC,AB, product by SUEZ [43]. It is part of the SeaPRO series of seawater desalination systems that highlights low energy consumption with a variable frequency drive for high pressure and boost pumps. The selected model also includes pre-filter, post-filter, primary and final pressure gauges, and a flow control centre including concentrate and recycle valves. The technical specifications of this plant are shown in Table 1, in which the power consumption of the whole treatment process (pre-treatment, main desalination, post treatment) was taken from an equivalent containerized system (i.e., the “SeaTECH-12”, a 163 m³/day integrated container).

In this study, only two variations were considered:

1. A motor voltage of 220 V instead of the original 380 V, to be compatible with the output voltage of the OBREC pico-turbines;
2. An increased value of energy consumption, moving from the proposed 1.9 kWh/mc to 2.1 kWh/mc, i.e., a 10% increase in order to provide a more conservative estimation of fresh water outflow.

It is worth noting that the selected average energy consumption is in any case greater, and hence precautionary, than the one found by Folley et al. [44] over a wide range of sea-water feed conditions.

Table 1. Technical specifications of the reverse osmosis system.

Equipment	Specification
Recovery	45%
Number of membranes	16
Nominal product flow	9.085 m ³ /h
Motor power	380 VAC, 3 phases, 50 Hz
Control circuit	220 V, single phase, 50 Hz
Power consumption	1.9 kWh/m ³

3. Results

3.1. Offshore Wave Power

The wave climate parameters and the assessment of the monthly and yearly mean wave power based on the 20-year average are shown in Table 2. The annual wave power was found to be 12.86 kW/m. The results are graphically represented with polar diagrams assembled in Figure 6. This value is not high, as expected. In fact, despite the very long fetch along the wave sector, the region of the central Indian ocean is poor of strong storms conditions [29,45,46]. However,

an important characteristic of such a wave climate is a relative low monthly, seasonal and interannual variability. This is due to the South Equatorial Current, which impinges on the coast of Madagascar as a single broad current at about 15° S. The highest seasonal variation is smoothed due to the presence of the blocking effect of the Seychelles–Mauritius Ridge (at latitude 60° E) on the annual Rossby wave [47,48] generated by the wind stress curl in the east [49]. In fact, a relatively small standard deviation of significant wave height, mean period and wave power are found (Table 2). In particular the mean percentage of power provided by Spring, Summer, Autumn and Winter are 19%, 19%, 25% and 37% respectively. The 20-year average monthly distributions of the minimum, mean and maximum significant wave height are shown in Figure 7.

Table 2. Main wave climate parameters (based on the 20-year average) at ECMWF grid points.

Month	$H_{s,mean}$ (m)	$H_{s,max}$ (m)	$H_{s,min}$ (m)	σ_H (m)	$T_{m,mean}$ (s)	$T_{m,max}$ (s)	σ_T (s)	P_{mean} (kW)
January	1.87	3.09	0.46	0.30	8.28	9.40	0.60	18.67
February	1.95	3.10	0.49	0.32	8.27	9.70	0.58	19.63
March	1.72	2.83	0.50	0.21	8.10	9.47	0.66	14.59
April	1.30	2.51	0.15	0.30	8.02	9.77	0.69	8.77
May	1.14	1.91	0.16	0.28	7.71	9.36	0.63	6.50
June	1.26	2.73	0.42	0.18	7.74	9.46	0.74	8.76
July	1.36	3.05	0.21	0.27	8.33	10.43	0.86	11.38
August	1.17	2.68	0.04	0.36	8.15	9.96	0.82	8.52
September	1.20	2.68	0.13	0.24	8.05	9.61	0.69	9.20
October	1.39	2.75	0.04	0.40	8.42	10.59	0.87	12.10
November	1.68	3.35	0.06	0.49	8.46	10.81	0.83	17.87
December	1.73	3.21	0.10	0.42	8.34	10.34	0.74	18.31
Mean	1.48	2.82	0.23	0.32	8.15	9.91	0.72	12.86
σ	0.29	0.38	0.18	0.09	0.24	0.51	0.10	4.73

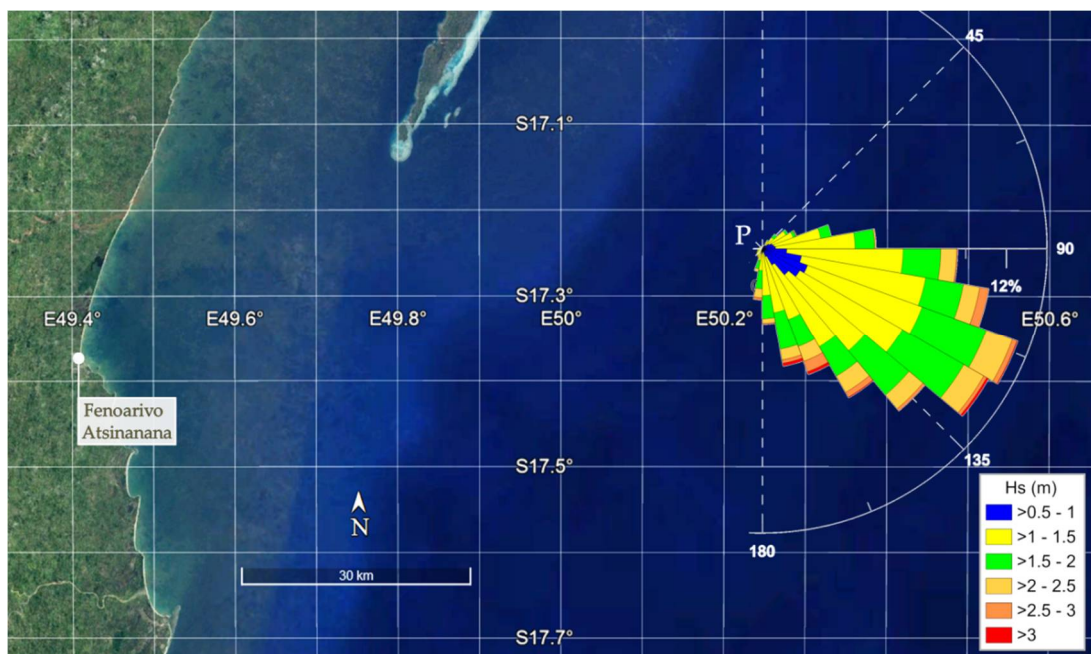


Figure 6. Wave climate for the ECMFW grid points.

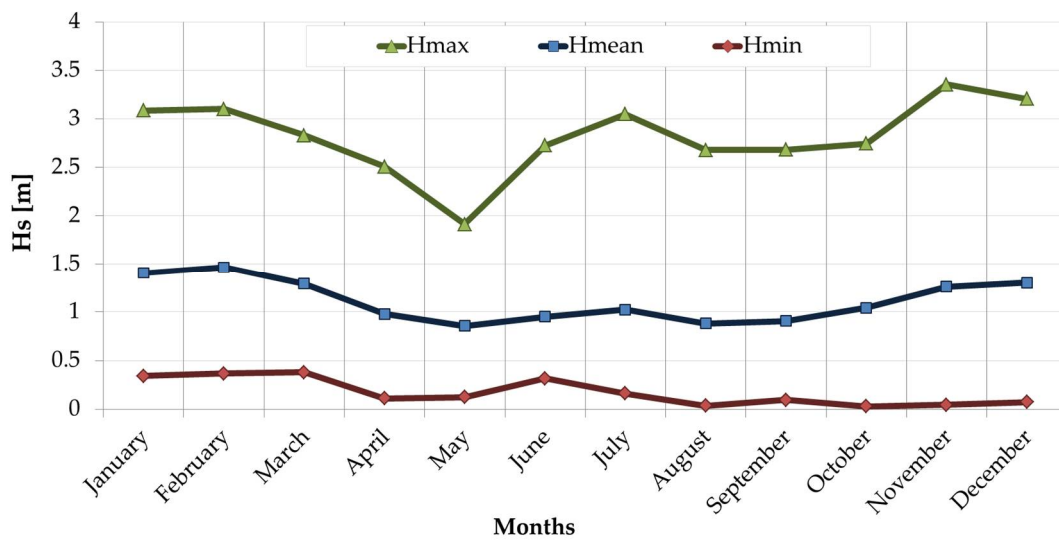


Figure 7. Monthly distribution of the minimum, mean and maximum significant wave height averaged over 20 years at ECMWF grid point P.

3.2. Inshore Wave Pattern at the Study Site

Due to the energy loss in shallow water, the mean nearshore power in front of the breakwater was found to range between 9.95 kW/m (January) and 3.3 kW/m (May), corresponding to a standard deviation of 2.2 kW/m from the mean of 6.27 kW (20-year average), as shown in Table 3. The wave sector decreased significantly to a width of 75°, ranging between the directions 55° N and 130° N. Figure 8 shows the seasonal distribution of the wave height patterns.

Table 3. Monthly and yearly wave power (based on the 20-year average) at the study site at 5 m isobath.

Month	H _{s,mean} (m)	H _{s,max} (m)	H _{s,min} (m)	σ _H (m)	T _{m,mean} (s)	T _{m,max} (s)	σ _T (s)	P _{mean} (kW)
January	1.58	2.12	2.50	0.27	7.62	8.65	0.54	9.95
February	1.52	2.09	2.47	0.29	7.57	8.84	0.54	9.12
March	1.40	1.92	2.27	0.22	7.40	8.69	0.62	7.31
April	1.07	1.71	2.01	0.30	7.33	8.88	0.60	4.58
May	0.92	1.31	1.54	0.21	7.13	8.73	0.65	3.30
June	1.03	1.86	2.19	0.18	7.05	8.46	0.65	4.24
July	1.08	2.02	2.38	0.27	7.55	9.55	0.78	5.46
August	0.96	1.93	2.27	0.31	7.49	9.23	0.76	4.35
September	0.97	1.84	2.17	0.17	7.43	8.85	0.63	4.58
October	1.11	1.86	2.19	0.31	7.66	9.69	0.83	5.76
November	1.31	2.27	2.68	0.47	7.73	9.90	0.78	8.40
December	1.34	2.13	2.51	0.33	7.57	9.33	0.62	8.18
Mean	1.19	1.92	2.27	0.28	7.46	9.07	0.67	6.27
σ	0.23	0.25	0.29	0.08	0.21	0.46	0.10	2.22

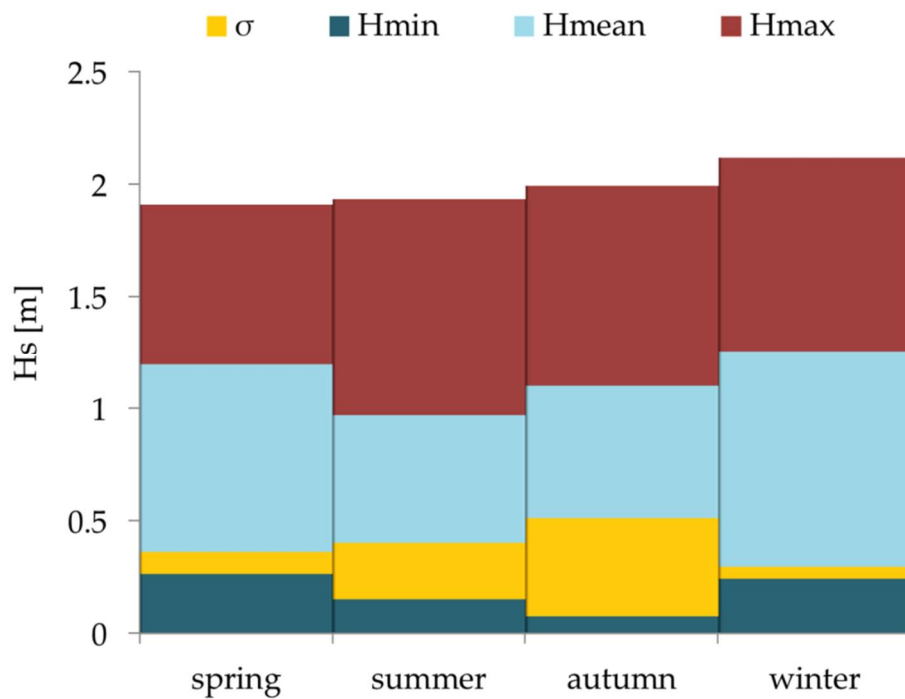


Figure 8. Seasonal wave climate characterization, in terms of significant wave height, averaged over 20 years at the study site.

3.3. Wave-to-Wire Production and Freshwater Outflow

Following the inshore wave energy assessment, the effective power production of OBREC was computed.

Firstly, the optimal geometry and turbine strategy were found. In fact, the optimization procedure provided a crest level of 1.95 m, a reservoir cross-section width of 4.8 m and an OBREC single module length of 10 m. Each module was equipped with 20 turbine complete generator sets (i.e., two turbines, each 1 m in length). The average effective output power was 2.31 kW/module and the yearly produced energy was found to be 20,250 kWh/year. Considering the 50 constituent parts of the whole OBREC breakwater of 500 m, the total power was 115.5 kW, corresponding to about 1.01 GWh/year. The power production data are summarized in Table 4, together with the fresh water outflow. In particular, a total amount of 482,142 mc/year was estimated. This means that in Fenoarivo Atsinanana, a city of 21,036 inhabitants [50], the freshwater supplied by the 500 m long OBREC-driven desalination plant could provide an average of about 63 L per capita per day. Considering that Fenoarivo is one of the poorest cities in the world and that the average availability of water for a Madagascar citizen is less than 10 L per day [51], the results here obtained are very positive and advantageous. Figure 9 shows the monthly production of fresh water, averaged on 20 years of wave data. The figure also shows the recommended values of the water requirements for different uses [52]. The amount of water supplied by the system represents a large enough quantity for all physiological needs.

Table 4. Summary of the results.

Description	Units	Value
Length of breakwater	[m]	500
Effective module average power	[kW]	2.31
Average overtopping water	[m ³ /yr]	725,328,011
Number of OBREC modules	[-]	50
Total energy production	[MWh/yr]	1012.5
Power consumption	[kWh/m ³]	2.1
Water treated	[m ³ /yr]	87,662,338
Water post-treated (desalinated)	[m ³ /yr]	482,143
Inhabitants	[-]	21,036
Yearly outflow per capita	[m ³ /pc/yr]	22,919.89
Litres per capita per day	[L/pc/day]	62.79

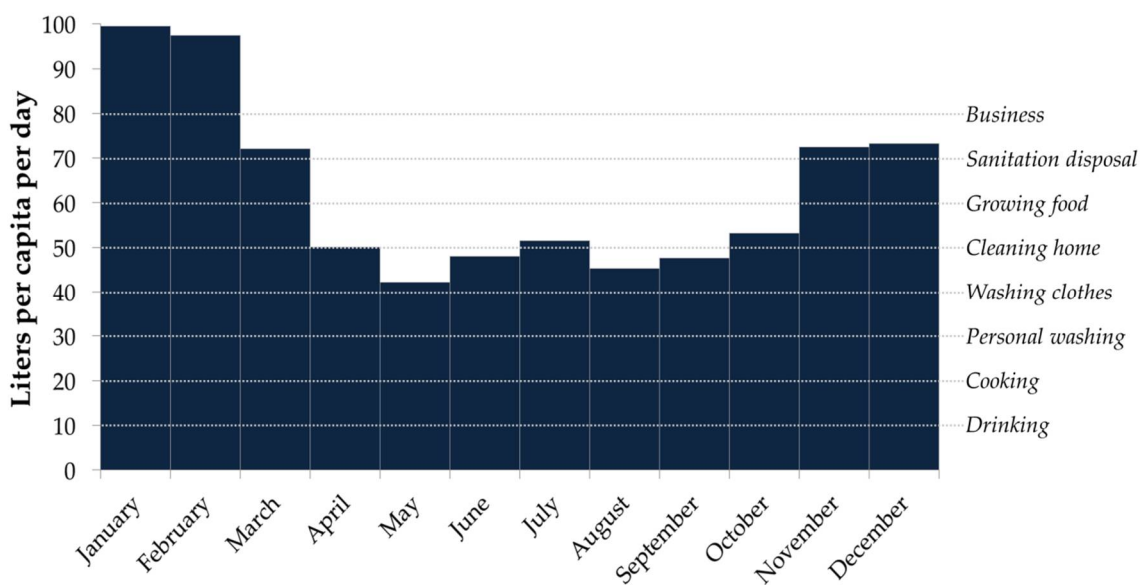


Figure 9. Seasonal distribution of freshwater production and hierarchy of water requirements.

4. Additional Considerations

Some key technological finding can be extracted from previous paragraphs. First, it is worth highlighting that the final desalinated water is about 6% of the total overtopping water collected by the system and used to generate electricity (see comparison between third and eighth row in Table 4). This may not seem like much. However, this also means that the brine and overtopping water not used in the desalination process are discharged together, hence the highly-concentrated salt solution can be quickly dispersed and its effect on the environment can be minimised. In fact, the mixing functions in the ocean are such that it will not harm marine life unless there is no mixing at the release point, which is avoided.

The second point concerns the effective proportion of the time that an operating OBREC module is able to generate the required energy to cover the energy demand of the desalination unit. From the simulations, it was found that the OBREC system was operative for more than 52% of the time during the year, corresponding to 190 operating days. This value is strongly interesting compared to other renewable energy sources, but it could be misinterpreted. In fact, a significant proportion of the wave energy production is provided during storm (also mild storm) conditions and the percentage of “calm” sea state (wave climate characterized by wave height less than 0.5 m) was found on average to be 16.7%. Therefore, in order to provide an adequate constant supply of freshwater production, connecting the

system to the grid is strongly recommended. Obviously, the overproduction of electricity during major storms (i.e., exceeding consumption) will be fed into the grid; the buyback of the excess electricity rate should outweigh the requests for electricity from the grid during wave conditions that are unable to ensure turbine operation at full capacity.

The results on water production obtained in this work cannot be placed clearly in context with the results of other studies. In fact, the data available for other wave-energy-based desalination prototype installations are provided without mentioning the wave energy pattern or the overall dimensions of the prototype, making any comparison difficult [53].

Some brief overall considerations about the advantages of integration between the OBREC and RO desalination plant into a traditional coastal defence structure are summarised here:

- Low marginal costs compared to building traditionally-conceived breakwaters, as the OBREC system has a very low (<5 years) payback period [23], and the ex-works price of the investigated SeaPRO desalination unit is about € 180,000 [43];
- Low marginal environmental impact, unlike traditional structures [54,55];
- Ease of access for construction and maintenance of the equipment [56];
- Effective in countering erosive trends [57–59];
- Recirculation of excess water collected from the reservoir behind the breakwater, i.e., inside the harbour, making projects more acceptable in the long run and more suitable for the marine environment [60].

The last consideration regards the reliability of the system proposed. It is built as a robust concrete structure with the turbine shaft and the gates controlling the water flow being virtually the only moving parts in the mechanical system. The structure is safe even with the malfunctioning of these moving parts. The turbines and water treatment system are well-tested, mass-produced technologies. All the hydro–electro–mechanical equipment is contained in the machine room. Such conditions provide confidence in the high reliability of the system.

5. Conclusions

This work seeks to address the technical challenges of suitable and sustainable freshwater production using wave energy.

Therefore, the application of a reverse osmosis system to the OBREC technology was analysed in a location in Madagascar that is effectively experiencing a water shortage situation, with a hypothesised new coastal structure.

A conservative freshwater production of 964.3 mc per meter wave front was provided. The 500 m long OBREC breakwater was able to supply more than 60 L per capita per day for all the inhabitants of Fenoarivo Atsinanana. These results seem promising, but more detailed information on alternative wave-powered desalination technologies are required in order to allow for benchmarking and overlapping with onsite wave power data, and the detailed screening of the site specific desalination plant. The approach proposed here is not intended to replace or substitute the need for a comprehensive feasibility study.

Generally speaking, the data demonstrate that if a new breakwater for coastal or marina protection is needed in an area similar to the wave climate of north-eastern Madagascar, a multifunctional coastal defence equipped with a WEC/desalination unit could be a viable alternative. In the feasibility analysis, in fact, the sharing of construction costs and the overall benefits related to electricity/freshwater production should be highlighted an enhance of the breakwater's use value. Finally, the relatively low marginal environmental impact of the operating system (being a build-integrated solution) should provide broader community acceptance.

Author Contributions: P.C. conceived the paper and carried out the elaborations. D.V. revised the paper draft and P.C. updated the paper according to his review.

Acknowledgments: The numerical model OBRECSim and experimental analysis were developed during the National Operational Programme for Research and Competitiveness 2007–2013 (NOP for R&C) founded project PON04a3_00303 titled “DIMEMO-DIga Marittima per l’Energia del Moto Ondoso” (Maritime Breakwater for Wave Energy Conversion). Authors gratefully acknowledge the Italian Ministry of Education, University and Research (MIUR) for supporting this innovative research.

Conflicts of Interest: The authors declare no conflict of interest.

References

1. Gilau, A.M.; Small, M.J. Designing cost-effective sea water reverse osmosis system under optimal energy options for developing countries. In Proceedings of the International Conference on Renewable Energy for Developing Countries, Washington, DC, USA, 5–7 April 2006; p. 1.
2. International Desalination Association. Available online: <http://idadesal.org/desalination-101/desalination-by-the-numbers/> (accessed on 10 April 2018).
3. Eltawil, M.A.; Zhengming, Z.; Yuan, L. Renewable energy powered desalination systems: Technologies and economics-state of the art. In Proceedings of the 12th International Water Technology Conference, Alexandria, Egypt, 27–30 March 2008; pp. 27–30.
4. Mathioulakis, E.; Belessiotis, V.; Delyannis, E. Desalination by using alternative energy: Review and state-of-the-art. *Desalination* **2007**, *203*, 346–365. [[CrossRef](#)]
5. Miller, S.; Shemer, H.; Semiat, R. Energy and environmental issues in desalination. *Desalination* **2015**, *366*, 2–8. [[CrossRef](#)]
6. Shouman, E.R.; Sorour, M.H.; Abulnour, A.G. Economics of Renewable Energy for Water Desalination in Developing Countries. *J. Eng. Sci. Technol. Rev.* **2015**, *8*, 227–231. [[CrossRef](#)]
7. El-Samanoudi, M.A.; Abd-Rabbo, M.F.; Sarhan, A.A.; Attia, M. Impact of Water Desalination Technologies on Environmental Development. In Proceedings of the Seventh International Water Technology Conference Egypt, Cairo, Egypt, 1–3 April 2003; Volume 1.
8. Drioli, E.; Ali, A.; Macedonio, F. Membrane operations for process intensification in desalination. *Appl. Sci.* **2017**, *7*, 100. [[CrossRef](#)]
9. Water Desalination Using Renewable Energy. Available online: https://iea-etsap.org/E-TechDS/PDF/I12IR_Desalin_MI_Jan2013_final_GSOK.pdf (accessed on 10 April 2018).
10. Davies, P.A. Wave-powered desalination: Resource assessment and review of technology. *Desalination* **2005**, *186*, 97–109. [[CrossRef](#)]
11. Pleass, C.M. The use of Wave Powered Seawater Desalination Systems. In Proceedings of the International Symposium on Wave and Tidal Energy, Canterbury, UK, 27–29 September 1974.
12. Hicks, D.C.; Mitcheson, G.R.; Pleass, C.M.; Salevan, J.F. Delbouy: Ocean wave-powered seawater reverse osmosis desalination systems. *Desalination* **1989**, *73*, 81–94. [[CrossRef](#)]
13. Charcosset, C. A review of membrane processes and renewable energies for desalination. *Desalination* **2009**, *245*, 214–231. [[CrossRef](#)]
14. Sharmila, N.; Jaliha, P.; Swamy, A.K.; Ravindran, M. Wave powered desalination system. *Energy* **2004**, *29*, 1659–1672. [[CrossRef](#)]
15. AquaEnergy, The AquaBuoy Wave Energy Converter. 2006. Available online: <http://aquaenergygroup.com> (accessed on 14 November 2006).
16. The CETO Wave Energy Converter. Available online: <http://www.cornwallislesofscillygrowthprogramme.org.uk/growth-story/ceto-wave-energy/> (accessed on 10 April 2018).
17. Ocean Motion International WavePump Performance Test, FINAL REPORT. 2013. Available online: <http://oceanmotionintl.com/wp-content/uploads/2014/09/A.3.pdf> (accessed on 10 April 2018).
18. Alkaisi, A.; Mossad, R.; Sharifian-Barforoush, A. A review of the water desalination systems integrated with renewable energy. *Energy Procedia* **2017**, *110*, 268–274. [[CrossRef](#)]
19. Ali, A.; Tufa, R.A.; Macedonio, F.; Curcio, E.; Drioli, E. Membrane technology in renewable-energy-driven desalination. *Renew. Sustain. Energy Rev.* **2018**, *81*, 1–21. [[CrossRef](#)]
20. Abdel-Aal, E.A.; Farid, M.E.; Hassan, F.S.; Mohamed, A.E. Desalination of Red Sea water using both electro dialysis and reverse osmosis as complementary methods. *Egypt. J. Pet.* **2015**, *24*, 71–75. [[CrossRef](#)]
21. What We Do. Available online: <http://wateraid.com> (accessed on 21 October 2017).

22. Faure, M.; Rakotomalala, O.; Pelon, R. *Economic Contributions from Industrial Mining in Madagascar: Research Summary (English)*; World Bank Group: Washington, DC, USA, 2015.
23. Contestabile, P.; Di Lauro, E.; Buccino, M.; Vicinanza, D. Economic assessment of Overtopping Breakwater for Energy Conversion (OBREC): A case study in Western Australia. *Sustainability* **2016**, *9*, 51. [CrossRef]
24. Contestabile, P.; Ferrante, V.; Vicinanza, D. Wave Energy Resource along the Coast of Santa Catarina (Brazil). *Energies* **2015**, *8*, 14219–14243. [CrossRef]
25. Contestabile, P.; Ferrante, V.; Di Lauro, E.; Vicinanza, D. Prototype Overtopping Breakwater for Wave Energy Conversion at Port of Naples. In Proceedings of the 26th International Conference ISOPE, Rhodes, Greece, 26 June–2 July 2016; pp. 616–621.
26. Vicinanza, D.; Contestabile, P.; Nørgaard, J.; Lykke Andersen, T. Innovative rubble mound breakwaters for overtopping wave energy conversion. *Coast. Eng.* **2014**, *88*, 154–170. [CrossRef]
27. European Centre for Medium-Range Weather Forecasts. Available online: <http://www.ecmwf.int/> (accessed on 10 April 2018).
28. Goda, Y. *Random Waves and Design of Maritime Structures*, 2nd ed.; World Scientific: Singapore, 2000.
29. Contestabile, P.; Lauro, E.D.; Galli, P.; Corselli, C.; Vicinanza, D. Offshore Wind and Wave Energy Assessment around Malé and Magoodhoo Island (Maldives). *Sustainability* **2017**, *9*, 613. [CrossRef]
30. ABP Marine Environmental Research Ltd. *Atlas of UK Marine Renewable Energy Resources: Technical Report*; Report No. R.1106 Prepared for the UK Department of Trade and Industry; ABP Marine Environmental Research Ltd.: Southampton, UK, 2004.
31. MIKE 21. Available online: <http://www.mikepoweredbydhi.com/products/mike-21> (accessed on 10 April 2018).
32. Holthuijsen, L.H.; Booij, N.; Herbers, T.H.C. A prediction model for stationary, short-crested waves in shallow water with ambient currents. *Coast. Eng.* **1989**, *13*, 23–54. [CrossRef]
33. The General Bathymetric Chart of the Oceans. Available online: <http://www.gebco.net/> (accessed on 10 April 2018).
34. Navionics. Available online: <http://www.navionics.com/> (accessed on 10 April 2018).
35. Iuppa, C.; Contestabile, P.; Cavallaro, L.; Foti, E.; Vicinanza, D. Hydraulic performance of an innovative breakwater for overtopping wave energy conversion. *Sustainability* **2016**, *8*, 1226. [CrossRef]
36. Electway-Store. Available online: <http://www.electway.net/upload/file/1362219611.pdf> (accessed on 10 March 2018).
37. Van der Bruggen, B.; Vandecasteele, C. Distillation vs. membrane filtration: Overview of process evolutions in seawater desalination. *Desalination* **2002**, *143*, 207–218. [CrossRef]
38. Buross, O.K. *The ABCs of Desalting*; International Desalination Association: Topsfield, MA, USA, 2000; p. 30.
39. Contestabile, P.; Aristodemo, F.; Vicinanza, D.; Ciavola, P. Laboratory Study on a Beach Drainage System. *Coast. Eng.* **2012**, *66*, 50–64. [CrossRef]
40. Ciavola, P.; Vicinanza, D.; Aristodemo, F.; Contestabile, P. Large-scale morphodynamic experiments on a beach drainage system. *J. Hydraul. Res.* **2011**, *49*, 523–528. [CrossRef]
41. Ciavola, P.; Contestabile, P.; Aristodemo, F.; Vicinanza, D. Beach sediment mixing under drained and undrained conditions. *J. Coast. Res.* **2013**, *65*, 1503–1508. [CrossRef]
42. Ciavola, P.; Vicinanza, D.; Fontana, E. Beach drainage as a form of shoreline stabilization: Case studies in Italy. In Proceedings of the 31st International Conference, Hamburg, Germany, 31 August–5 September 2008; Volume 5, pp. 2646–2658.
43. Suez Water Technologies. Available online: <http://engg.suezwatertechnologies.com/products/configurator> (accessed on 10 March 2018).
44. Folley, M.; Suarez, B.P.; Whittaker, T. An autonomous wave-powered desalination system. *Desalination* **2008**, *220*, 412–421. [CrossRef]
45. Swallow, J.; Fieux, M.; Schott, F. The boundary currents east and north of Madagascar: 1. Geostrophic currents and transports. *J. Geophys. Res. Oceans* **1988**, *93*, 4951–4962. [CrossRef]
46. Schott, F.; Fieux, M.; Kindle, J.; Swallow, J.; Zantopp, R. The boundary currents east and north of Madagascar: 2. Direct measurements and model comparisons. *J. Geophys. Res. Oceans* **1988**, *93*, 4963–4974. [CrossRef]
47. Rossby, C.G. Relation between variations in the intensity of the zonal circulation of the atmosphere and the displacements of the semi-permanent centers of action. *J. Mar. Res.* **1939**, *2*, 38–55. [CrossRef]

48. Platzman, G.W. The Rossby wave. *Q. J. R. Meteorol. Soc.* **1968**, *94*, 225–248. [CrossRef]
49. Jamart, B.M.; Nihoul, J.C.J. (Eds.) *Mesoscale/synoptic Coherent Structures in Geophysical Turbulence*; Elsevier: Amsterdam, The Netherlands, 1989; Volume 50.
50. World Population Review. Available online: <http://worldpopulationreview.com/countries/madagascar-population/cities/> (accessed on 10 April 2018).
51. African Development Bank Group. Available online: https://www.afdb.org/fileadmin/uploads/afdb/Documents/Project-and-Operations/Madagascar_-_The_Grand_Sud_Rural_Potable_Water_and_Sanitation_Project_-_Appraisal_Report.pdf (accessed on 10 March 2018).
52. World Health Organization. Available online: http://www.who.int/water_sanitation_health/publications/2011/WHO_TN_09_How_much_water_is_needed.pdf?ua=1 (accessed on 10 April 2018).
53. Leijon, J.; Boström, C. Freshwater production from the motion of ocean waves—A review. *Desalination* **2018**, *435*, 161–171. [CrossRef]
54. Vicinanza, D.; Nørgaard, J.H.; Contestabile, P.; Andersen, T.L. Wave loadings acting on overtopping breakwater for energy conversion. *J. Coast. Res.* **2013**, *65*, 1669–1674. [CrossRef]
55. Buccino, M.; Stagonas, D.; Vicinanza, D. Development of composite sea wall wave energy converter system. *Renew. Energy* **2015**, *81*, 509–522. [CrossRef]
56. Iuppa, C.; Cavallaro, L.; Foti, E.; Vicinanza, D. Potential wave energy production by different wave energy converters around Sicily. *J. Renew. Sustain. Energy* **2015**, *7*, 1–16. [CrossRef]
57. Abanades, J.; Greaves, D.; Iglesias, G. Coastal defence using wave farms: The role of farm-to-coast distance. *Renew. Energy* **2014**, *75*, 572–582. [CrossRef]
58. Abanades, J.; Greaves, D.; Iglesias, G. Wave farm impact on beach modal state. *Mar. Geol.* **2015**, *361*, 126–135. [CrossRef]
59. Abanades, J.; Flor-Blanco, G.; Flor, G.; Iglesias, G. Dual wave farms for energy production and coastal protection. *Ocean Coast. Manag.* **2018**, *160*, 18–29. [CrossRef]
60. Azzellino, A.; Contestabile, P.; Ferrante, V.; Lanfredi, C.; Vicinanza, D. Strategic environmental assessment to evaluate WEC projects in the perspective of the environmental cost-benefit analysis. In Proceedings of the International Offshore and Polar Engineering Conference, Maui, HI, USA, 19–24 June 2011; ISOPE: Maui, HI, USA, 2011; pp. 709–715.



© 2018 by the authors. Licensee MDPI, Basel, Switzerland. This article is an open access article distributed under the terms and conditions of the Creative Commons Attribution (CC BY) license (<http://creativecommons.org/licenses/by/4.0/>).